Petković, J., Žegura, B., Stevanović, M., Drnovšek, N., Uskoković, D., Novak, S., Filipič, M., 2011. DNA damage and alterations in expression of DNA damage responsive genes induced by TiO_2 nanoparticles in human hepatoma HepG2 cells. Nanotoxicology 5, 341–353. https://doi.org/10.3109/17435390.2010.507316

DNA damage and alterations in expression of DNA damage responsive genes induced by TiO_2 nanoparticles in human hepatoma HepG2 cells

JANA PETKOVIĆ[1], BOJANA ŽEGURA[1], MAGDALENA STEVANOVIĆ[2], NATAŠA DRNOVŠEK[3], DRAGAN USKOKOVIĆ[2], SAŠA NOVAK[3], & METKA FILIPIČ[1]

[1]*Department of Genetic Toxicology and Cancer Biology, National Institute of Biology, Ljubljana, Slovenia,* [2]*Institute of Technical Sciences of the Serbian Academy of Sciences and Arts, Belgrade, Serbia, and* [3]*Department for Nanostructured Materials, Jožef Stefan Institute, Jamova 39, Ljubljana, Slovenia*

(Received 3 March 2010; accepted 6 July 2010)

Abstract

We investigated the genotoxic responses to two types of TiO_2 nanoparticles (<25 nm anatase: TiO_2-An, and <100 nm rutile: TiO_2-Ru) in human hepatoma HepG2 cells. Under the applied exposure conditions the particles were agglomerated or aggregated with the size of agglomerates and aggregates in the micrometer range, and were not cytotoxic. TiO_2-An, but not TiO_2-Ru, caused a persistent increase in DNA strand breaks (comet assay) and oxidized purines (Fpg-comet). TiO_2-An was a stronger inducer of intracellular reactive oxygen species (ROS) than TiO_2-Ru. Both types of TiO_2 nanoparticles transiently upregulated mRNA expression of *p53* and its downstream regulated DNA damage responsive genes (*mdm2, gadd45α, p21*), providing additional evidence that TiO_2 nanoparticles are genotoxic. The observed differences in responses of HepG2 cells to exposure to anatase and rutile TiO_2 nanoparticles support the evidence that the toxic potential of TiO_2 nanoparticles varies not only with particle size but also with crystalline structure.

Keywords: *TiO_2 nanoparticles, genotoxic, oxidative DNA damage, gene expression, HepG2 cells*

Introduction

The increasing use of nano-sized materials during the past several years has stimulated investigations of potential hazards of these useful materials for humans and environment. One of the most widely used nanoparticles (NPs) is composed of titanium dioxide (TiO_2); however, most of the titania powder is synthesized from the ore ilmenite, $FeTiO_3$ (Greenwood and Earnshaw 1997). TiO_2 particles larger than submicron-sized (>100 nm) have been classified as biologically inert in both humans and animals (Chen and Fayerweather 1988; Bernard et al. 1990; Hart and Hesterberg 1998) and are widely used as a white pigment in the production of paints, paper, plastics, ceramics, as a welding rod coating material and as a food additive (Nordman and Berlin 1986; Lomer et al. 2002; Gelis et al. 2003; Gurr et al. 2005). Strong absorption of UV light makes TiO_2 a very effective sunscreen for use in cosmetics (Gelis et al. 2003). Because of its photocatalytic properties, TiO_2 is applied in natural and waste water treatment as a disinfectant (Cho et al. 2004). TiO_2 finds applications in therapeutic purposes, being used as a photosensitizer for photodynamic therapy of endobronchial and esophageal cancers (Ackroyd et al. 2001). Nowadays, with the rapid development and advantages of nanotechnology, NPs of TiO_2 (<100 nm) are increasingly replacing their larger counterparts, predominantly because of their high stability, anticorrosion and better photocatalytic properties (Lomer et al. 2002; Gelis et al. 2003; Wang et al. 2007a). However, nanomaterials may differ from the bulk materials, not only in terms of their desirable properties but also in terms of their potential adverse effects.

TiO_2 NPs can cause oxidative stress-mediated toxicity in various tissues and cell types (Zhang and Sun 2004; Gurr et al. 2005; Hussain et al. 2005; Long et al. 2006; Xia et al. 2006), including DNA damage (Dunford et al. 1997; Rahman et al. 2002; Gurr et al. 2005; Wang et al. 2007a, 2007b), inflammation (Borm et al. 2000; Hohr et al. 2002; Warheit et al.

Correspondence: Dr Metka Filipič, Department of Genetic Toxicology and Cancer Biology, National Institute of Biology, SI-1000 Ljubljana, Slovenia. Tel: +386 5 9232 861. Fax: +386 1 257 38 47. E-mail: metka.filipic@nib.si

2006; Grassian et al. 2007), fibrosis (Baggs et al. 1997) and pulmonary damage (Bermudez et al. 2002, 2004; Park et al. 2009). Most of the toxicological studies of TiO_2 NPs in mammals have addressed their adverse effects upon exposure by inhalation and, on this basis TiO_2 has been classified by the International Agency for Research on Cancer (IARC) as an IARC Group 2B carcinogen "possibly carcinogenic to humans" upon inhalation (IARC 2006). However, oral ingestion is an important exposure route for the general population since TiO_2 is used as a food additive, in food contact materials, in toothpaste, capsules, etc. A literature survey revealed only one toxicokinetic study on oral exposure to TiO_2 NPs. TiO_2 NPs administered as single high-dose gavage (5 g/kg bw) to mice were shown to accumulate predominantly in the liver and spleen, while pathological changes were observed in kidney, liver and heart, along with changes in serum biochemical parameters such as increased lactate dehydrogenase and α-hydroxybutyrate dehydrogenase levels (Wang et al. 2007a). A recent study on the tissue distribution of intravenously (5 mg/kg body weight) administered TiO_2 NPs (>10 wt. % less than 100 nm size) to rats showed their highest levels on day one in all organs. The elevated TiO_2 levels were retained in the liver for 28 days, in the spleen there was a slight decrease in TiO_2 levels from day 1 to days 14 and 28, and in the lung and kidney the levels returned to control levels by day 14. There were no detectable levels of TiO_2 in blood cells, plasma, brain, or lymph nodes and there were also no obvious toxic health effects, no immune response, and no change in organ function (Fabian et al. 2008).

The toxicokinetic studies indicated that liver appears to be the target of NP toxicity; therefore, we have applied the experimental model with human hepatoma HepG2 cells to evaluate the genotoxic potential of TiO_2 NPs. It has been shown that the biological activities of NPs depend on their physicochemical properties (such as size and crystalline structure), therefore genotoxicity of two types of TiO_2 NPs: <25 nm anatase TiO_2 particles (TiO_2-An) and <100 nm rutile TiO_2 particles (TiO_2-Ru) has been studied. By means of comet assay and its modified version with lesion specific DNA repair enzymes formamidopyrimidine-DNA glycosylase (Fpg) and endonuclease III (Endo III) that convert oxidized purines and pyrimidines to AP sites and strand breaks, respectively (Collins et al. 1996), we determined TiO_2 NPs induction of DNA strand breaks and oxidative DNA damage. In addition we investigated the effect of TiO_2 NPs on mRNA expression of tumor suppressor gene *p53* and its downstream regulated DNA damage responsive genes, the cyclin-dependent kinase (CDK) inhibitor *p21,* the E3 ubiquitin ligase *mdm2,* and the growth arrest and DNA damage-inducible gene *gadd45*α.

Materials and methods

Chemicals

Eagle Minimal Essential Medium (EMEM), penicillin/streptomycin, L-glutamine, phosphate buffered saline (PBS), trypsin, fetal bovine serum, non-essential amino acid solution (100×), MTT (3-(4,5-dimethylthiazol-2-yl)-2,5-diphenyltetrazolium bromide), *tert*-butyl hydroperoxide (*t*-BOOH), benzo(a)pyrene (BaP), ethidium-bromide solution, 2,7-dichlorofluorescein diacetate (DCFH-DA), dimethyl sulfoxide (DMSO) were obtained from Sigma-Aldrich (St Louis, MO, USA). TRIzol was from Invitrogen (Carlsbad, USA), and cDNA High Capacity Archive Kit, TaqMan Universal PCR Master Mix and Taqman Gene Expression Assays from Applied Biosystems (Foster City, USA). Normal melting-point (NMP) agarose and low melting-point agarose (LMP) were from Gibco BRL (Paisley, Scotland, UK). Enzymes Fpg and Endo III were a gift from Dr Andrew R. Collins (Department of Nutrition, University of Oslo, Oslo, Norway).

Characteristics of TiO_2 nanoparticles

Two grades of TiO_2 powder with different average particles size (d <25 nm and d <100 nm) and crystalline structure (anatase and rutile) used in this study were obtained from Sigma-Aldrich (St Louis, MO, USA). We denoted them as TiO_2-An (Cat. no. 637254: anatase; particle size < 25 nm; 99.7% trace metals basis) and TiO_2-Ru (Cat. no. 637262: rutile; particle size ~ 10 × 40 nm; 99.5% trace metals basis). Their size, crystalline structure, specific surface area and aggregation or agglomeration were confirmed experimentally.

The size and morphology of TiO_2 NPs were observed by field-emission-gun scanning electron microscopy (FEG-SEM) JEOL 7600 F. The powder samples for the examination were coated with carbon (SCD 50 sputter coater). The crystal phase of the powders was identified by X-ray diffraction (XRD), using a Philips PW 1050 diffractometer with Cu-$KC_{1,2}$ radiation (Ni filter). Measurements were made in the range of 22 = 8–80° with scanning step width of 0.05° and time steps of 2s. UV/Vis (diffuse reflectance) spectroscopic characterization of the samples was recorded on GBC Cintra UV-Vis Spectrophotometer in the wavelength range of 200–800 nm. The specific surface area was determined by gas adsorption using the BET method (Gemini 2370, Micromeritics).

Particle size distribution of TiO_2 NPs in the treatment medium was measured by laser scattering, using a particle size distribution analyzer Horiba LA-920 (Japan). The particles were dispersed in EMEM medium at 30 μg/ml and sonicated using the same conditions as for preparation of particle suspensions for the cell treatments.

TiO_2 particles, stock solution and treatment media preparation

Powdered TiO_2 NPs were suspended in PBS at a concentration 1 mg/ml and sonicated for 30 min in an ultrasonic bath (Sonorex, Bandelin electronic, Germany) at a frequency of 60 kHz, voltage of 220 V and an electric current of 0.5 A to ensure uniform suspension. This stock solution was subsequently diluted in the complete cell growth medium to yield concentrations ranging from 1–250 μg/ml. These samples were then sonicated for 30 min to produce a stable, less-agglomerated nanocrystalline suspension before exposure of cells in culture.

Cell culture

HepG2 cells were obtained from European Collection of Cell Cultures (ECACC). Cells were grown in EMEM containing 10% fetal bovine serum, 1% non-essential amino acid solution, 2 mM L-glutamine and 100 U/ml penicillin plus 100 μg/ml streptomycin at 37°C in a humidified atmosphere with 5% CO_2.

Cytotoxicity assay

Cytotoxicity was determined with the MTT assay according to Mossman (1983) with minor modifications (Zegura et al. 2003). This assay measures the conversion of MTT to insoluble formazan by dehydrogenase enzymes of intact mitochondria of living cells. The HepG2 cells were seeded onto 96-well microplates (Nunc, Naperville, IL, USA) at a density of 40,000 cells/ml and incubated for 20 h at 37°C to attach. The medium was then replaced by fresh complete medium containing 0, 1, 10, 100 and 250 μg/ml of TiO_2 NPs, and incubated for 4, 24 and 48 h. In each experiment a vehicle control (cell growth medium containing 10% PBS) was included. MTT (final concentration 0.5 mg/ml) was then added, incubated for an additional 3 h, the medium with MTT was then removed and the formed formazan crystals dissolved in DMSO. The optical density (OD) was measured at 570 nm (reference filter 690 nm) using a microplate reading spectrofluorimeter (Tecan GENios, Austria). Viability was determined by comparing the OD of the wells containing the NPs treated cells with those of the vehicle (cell growth medium containing 10% PBS) treated cells. Five replicates per concentration point and three independent experiments were performed.

Intracellular ROS formation – DCFH-DA assay

The formation of intracellular ROS was measured using a fluorescent probe, DCFH-DA, as described by Osseni et al. (1999), with minor modifications (Zegura et al. 2004). DCFH-DA readily diffuses through the cell membrane and is hydrolyzed by intracellular esterases to non-fluorescent 2′,7′-dichlorofluorescein (DCFH) which, in the presence of ROS, is rapidly oxidized to highly fluorescent 2′,7′-dichlorofluorescein (DCF). The DCF fluorescence intensity is proportional to the amount of ROS formed intracellularly. H_2O_2 is the principle ROS responsible for the oxidation of DCFH-DA to DCF (LeBel et al. 1992).

The cells were seeded into 96-well, black, tissue culture treated microtiter plates (Nunc, Naperville, IL, USA) at a density of 75,000 cells/ml. After 20 h incubation at 37°C in 5% CO_2 the cells were loaded with 20 μM DCFH-DA for 30 min, DCFH-DA was then removed, and cells treated with 0, 1, 10, 100 and 250 μg/ml of TiO_2 NPs in PBS. Negative (non-treated cells) and positive (0.5 mM *t*-BOOH) controls were included in each experiment. For kinetic analysis of ROS formation the plates were maintained at 37°C and the fluorescence intensity (485 nm excitation/530 nm emission wavelengths) of the formed DCF recorded every 30 min during the 5 h incubation, using a microplate reading spectrofluorimeter (Tecan, Genios, Austria). Statistical significance between treated groups and controls was determined by two-tailed Student's *t*-test and $P < 0.05$ was considered as statistically significant. Three independent experiments with five replicates were performed.

Comet assay

HepG2 cells were seeded at a density of ≈ 60,000 cells/ml into 12-well microtiter plates (Corning Costar Corporation, Corning, NY, USA). After incubating the cells at 37°C in 5% CO_2 for 20 h to attach to the plates, the growth medium was replaced with fresh medium containing 0, 1, 10, 100 and 250 μg/ml TiO_2 NPs and incubated for 2, 4 and 24 h. In each experiment positive controls (0.5 mM *t*-BOOH and 50 μM BaP) and a vehicle control (cell growth medium containing 10% PBS) were included.

At the end of the exposure the cells were harvested and the DNA damage determined by the protocol of Singh et al. (1988) with minor modifications (Žegura and Filipič 2004). Images of 50 randomly selected nuclei per experimental point were analyzed with image analysis software Comet Assay IV (Perceptive Instruments, UK). Three independent experiments were performed for each of the treatment conditions. The percent of tail DNA was used to measure the level of DNA damage.

The level of oxidized purines/pyrimidines was determined with the modified comet assay as described by Collins et al. (1996). After the cell lysis the slides were washed three times for 5 min with endonuclease buffer (40 mM HEPES-KOH, 0.1 M KCl, 0.5 mM EDTA, 0.2 mg/ml bovine serum albumin, pH 8.0). Fifty microliter aliquots of Fpg/Endo III solution or enzyme buffer without Fpg/Endo III were added, covered with a cover glass and incubated at 37°C for 30/45 min. The slides were then processed as described above.

One-way analysis of variance (ANOVA, Kruskal-Wallis) was used to analyze the differences between treatments within each experiment. Dunnet's test was used for comparing median values of percentage tail DNA; $P < 0.05$ was considered as statistically significant.

mRNA expression analysis

Cells were seeded at a density of 1,000,000 on T-25 flasks (Corning Costar Corporation, Corning, NY, USA) and incubated for 20 h at 37°C and 5% CO_2 to attach. The growth medium was then replaced with fresh medium containing 0, 1, 10, and 100 μg/ml TiO_2 NPs and the cells incubated for 4 and 24 h. In each experiment a positive control (50 μM BaP) and a vehicle control (cell growth medium containing 10% PBS) were included. Total RNA from the cells was isolated using TRIzol reagent, and cDNA synthesized using 2 μg of total RNA and cDNA High Capacity Archive Kit (Applied Biosystems, CA, USA), according to the manufacturer's protocol. Gene expression of *p53, mdm2, gadd45*α and *p21* was quantified using real-time quantitative PCR (ABI 7900 HT Sequence Detection System, Applied Biosystems, USA). TaqMan Universal PCR Master Mix and the following Taqman Gene Expression Assays were used (all from Applied Biosystems): *p53* (tumor protein p53), Hs00153349_m1; *mdm2* (Mdm2, 'transformed 3T3 cell double minute 2', p53 binding protein gene), Hs00234753_m1; *gadd45*α ('growth arrest and DNA-damage-inducible gene, alpha'), Hs00169255_m1; and *p21* ('cyclin-dependent kinase inhibitor 1A') Hs00355782_m1. Amplification of GAPDH probe was performed as an internal control. The conditions for PCR were 50°C for 2 min, 95°C for 10 min and 40 cycles of 95°C for 15 s and 60°C for 1 min. The data obtained from Taqman Gene Expression Assays were analyzed using the ΔΔCt algorithm. Statistical significance between treated groups and controls was determined by two tailed Student's *t*-test and $P < 0.05$ was considered significant. Independent experiments were performed in duplicate and repeated at least three times.

Results

Characteristics of TiO_2 NPs

The characteristics of the TiO_2 nanopowders used in this study are summarized in Table I. The FEG-SEM examination of the TiO_2 nanopowders (Figures 1A–D) showed that both powders are aggregated, with nearly spherical crystallites for the TiO_2-An (Figures 1A, 1B) and elongated crystallites for the TiO_2-Ru (Figures 1C, 1D). The apparent average crystallite's sizes are in agreement with specified sizes provided by the manufacturer, i.e., around 25 nm for TiO_2-An and under 100 nm for the TiO_2-Ru, while the aggregates are much larger. The specific surface area was determined to be very similar for both powders, i.e., 129.3 m^2/g for TiO_2-An and 116.7 m^2/g for TiO_2-Ru, which is well in agreement with the producer's specifications (Table I). XRD confirmed crystalline structure for both, anatase sample and rutile sample of the TiO_2 NPs (Powder diffraction files). The X-ray diffractogram of rutile shows wider range of reflection and higher level of basic line related to X-ray diffractogram of anatase; which is indicating smaller crystallite size and lower degree of crystallinity of rutile. When Sherrer's formula for calculation the crystallite size was applied, the size of 10 nm was found for rutile on reflection (110) and of 15 nm for anatase on reflection (101). The reflectance UV spectra of the samples are in accordance with the reported values (Tryba 2008).

The particle size distribution determined by laser scattering particle size distribution analysis showed that in the medium both types of TiO_2 NPs are highly aggregated and agglomerated with an average size of aggregates and agglomerate size at the micron level (TiO_2-An: 915 ± 453 nm; TiO_2-Ru: 1542 ± 760 nm). However, the portion of submicron-sized particles is much lower in the case of the TiO_2-An than in TiO_2-Ru (Figure 1E). Micron-sized aggregates and agglomerates were confirmed also by FEG-SEM (Figures 1A–D).

Table I. Characteristics of the TiO_2 powders used in this study.

	Anatase TiO_2-An	Rutile TiO_2-Ru
Supplier information (Sigma-Aldrich)	Nanopowder, anatase crystalline structure, particle size <25 nm, surface area 200–220 m^2/g	Nanopowder, rutile crystalline structure, particle size ~10 nm × 40 nm, surface area 130–190 m^2/g
Measurements of specific surface area (BET)	129.3 m^2/g	116.7 m^2/g
FEG-SEM (supplied material) Particle size within the agglomerates/aggregates	<25 nm	<100 nm
Particle shape	Spherical crystallites	Elongated crystallites
XRD	Anatase type: tetragonal crystallographic system; $I4_1/amd$ space group (according to JCPDS: 21–1272); characteristic reflections (101) at 25.3; (200) at 48.0, 2θ	Rutile type: tetragonal crystallographic system; $P4_2/mnm$ space group (according to JCPDS: 34–0180); characteristic reflections (110) at 27.3; (101) at 36.0; (211) at 54.1, 2θ.
UV-Vis spectroscopy	Anatase: absorption peaks at λ_{max} = 300 nm and λ_{max} = 210 nm	Rutile: absorption peaks at λ_{max} = 305 nm and λ_{max} = 205 nm

FEG-SEM, field-emission-gun scanning electron microscope; XRD, X-ray diffraction; UV-Vis, ultraviolet- visible spectroscopy.

Cytotoxicity of TiO_2 NPs

The viability of HepG2 cells exposed to 0, 1, 10, 100 and 250 μg/ml of TiO_2-An or TiO_2-Ru for 4, 24 and 48 h was not significantly affected (data not shown). Therefore, these concentrations were used in further experiments.

Induction of intracellular ROS formation

To explore whether the TiO_2-An and TiO_2-Ru NPs induced DNA damage is associated with intracellular ROS formation, we measured the kinetics of their formation in HepG2 cells (Figure 2). After 5 h exposure, TiO_2-An induced a significant elevation of intracellular ROS formation at all applied concentrations, with a two-fold increase over control level at the highest concentration, while TiO_2-Ru induced a 1.4-fold elevation only at the highest concentration (Figure 2A). Kinetic measurement of the ROS formation during the 5 h exposure showed that the level of TiO_2-An induced ROS increased steadily over the control level, while TiO_2-Ru induced an increase in the ROS level during the first 90-min exposure, which afterwards increased at the same rate as the control (Figure 2B).

Induction of DNA strand breaks and oxidative DNA damage

In HepG2 cells exposed to TiO_2-An NPs we detected slight, however statistically significant ($P < 0.05$) greater amount of DNA strand breaks than in the control, as shown using the comet assay (Figure 3). The greater amount of DNA damage was observed at the highest concentration (250 μg/ml) after 2, 4 and 24 h exposure and after 4 h exposure also at 1 μg/ml. Exposure to TiO_2-Ru particles induced significantly more strand breaks only in cells exposed for 4 h to 100 μg/ml TiO_2-Ru.

The induction of oxidative DNA damage was studied with the modified comet assay with purified DNA damage specific enzymes, Fpg and Endo III, which recognize and excise oxidized purines and pyrimidines, respectively. The increase of % tail DNA in enzyme treated slides compared to buffer treated thus reflects the amount of oxidized nucleic bases.

In cells exposed to TiO_2-An we observed a significant dose-dependent increase of Fpg-sensitive sites at concentrations 10, 100 and 250 μg/ml after 2, 4 and 24 h (Figure 4A). The highest levels of Fpg-sensitive sites were observed after 4 h exposure at concentrations of 100 and 250 μg/ml, which declined slightly after 24 h exposure, but remained significantly different from the control at concentrations 10, 100 and 250 μg/ml. In cells exposed to TiO_2-Ru a significant increase of Fpg-sensitive sites was detected only after 24 h exposure to 10 and 100 μg/ml NPs (Figure 4B).

Induction of Endo III-sensitive sites by TiO_2 NPs was much lower than that of Fpg-sensitive sites and was not dose-dependent. After 2 h exposure to TiO_2-An, the increase of Endo III-sensitive sites was significant at the highest concentration (250 μg/ml), after 4 h of exposure at a concentration 100 μg/ml, and after 24 h of exposure at 10 μg/ml (Figure 5A). In cells exposed to TiO_2-Ru, we observed a significant

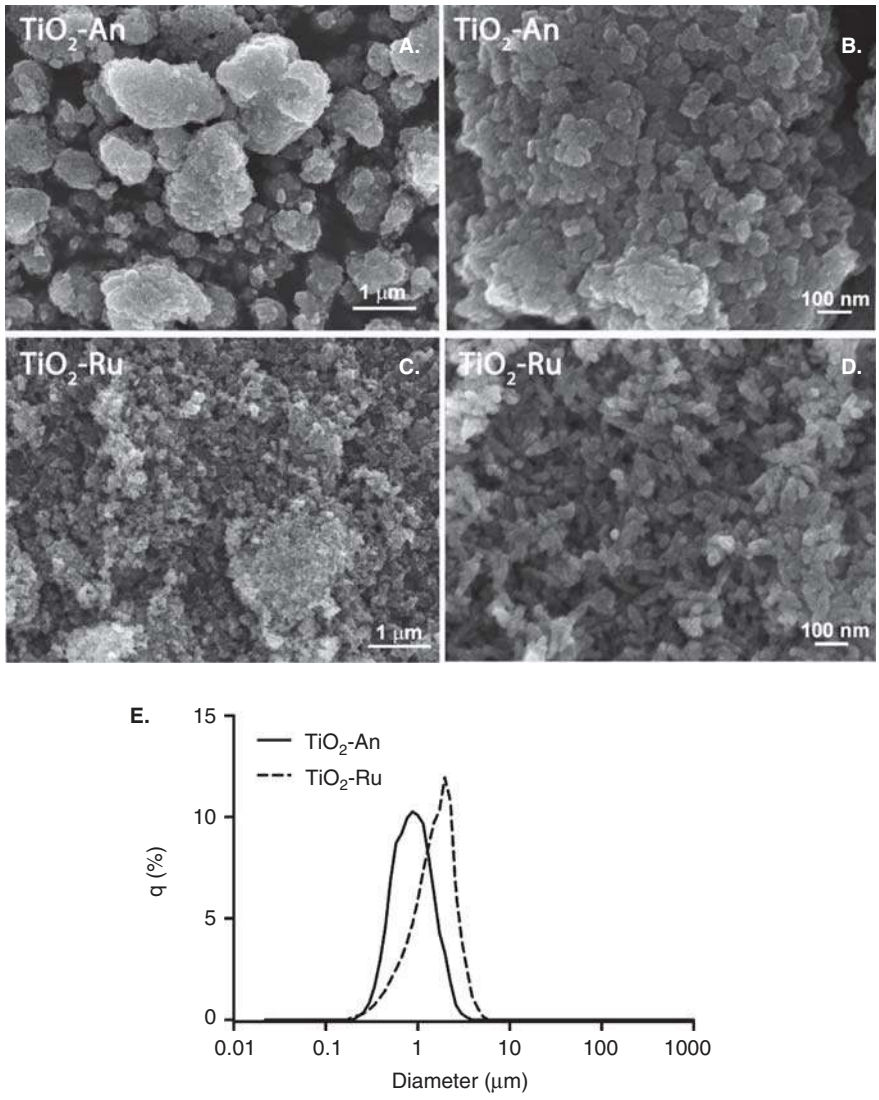

Figure 1. FEG-SEM images of the TiO_2-An (A, B) and TiO_2-Ru (C, D) NPs; Particle size distributions of TiO_2-An and TiO_2-Ru (E).

increase of Endo III-sensitive sites at the highest concentration (250 μg/ml) after 2 h and after 24 h exposure (Figure 5B).

Effect of TiO_2 NPs on the expression of DNA damage responsive genes

The mRNA expression of selected DNA damage responsive genes was analyzed after 4 h and 24 h exposure of HepG2 cells to 0, 1, 10 and 100 μg/ml of TiO_2-An and TiO_2-Ru by quantitative real-time PCR (Figure 6).

In cells exposed to TiO_2-An for 4 h (Figure 6A), the mRNA expression of *p53* was significantly greater than that of the control cells ($P < 0.05$) at the highest concentration (100 μg/ml). Under the same conditions, expression of *mdm2, p21* and *gadd45α* was not affected. After 24 h of exposure to TiO_2-An, the level of *p53* mRNA expression remained unchanged. The expression of *p21* and *mdm2* was significantly elevated at the highest concentration, while expression of *gadd45α* was significantly elevated at 10 and 100 μg/ml (Figure 6B).

In cells exposed to TiO_2-Ru the expression of *p53, mdm2, p21* and *gadd45α* after 4 h was significantly elevated at the highest concentration (100 μg/ml) (Figure 6C). After 24 h exposure to TiO_2-Ru, the expressions of *p21, mdm2* and *gadd45α* were significantly elevated at 10 and 100 μg/ml, while the expression of *p53* remained unchanged (Figure 6D).

As the positive control of the test system, we used 50 μM BaP. Exposure of HepG2 cells to BaP for 4 h did not affect expression of *p53, mdm2, p21* and

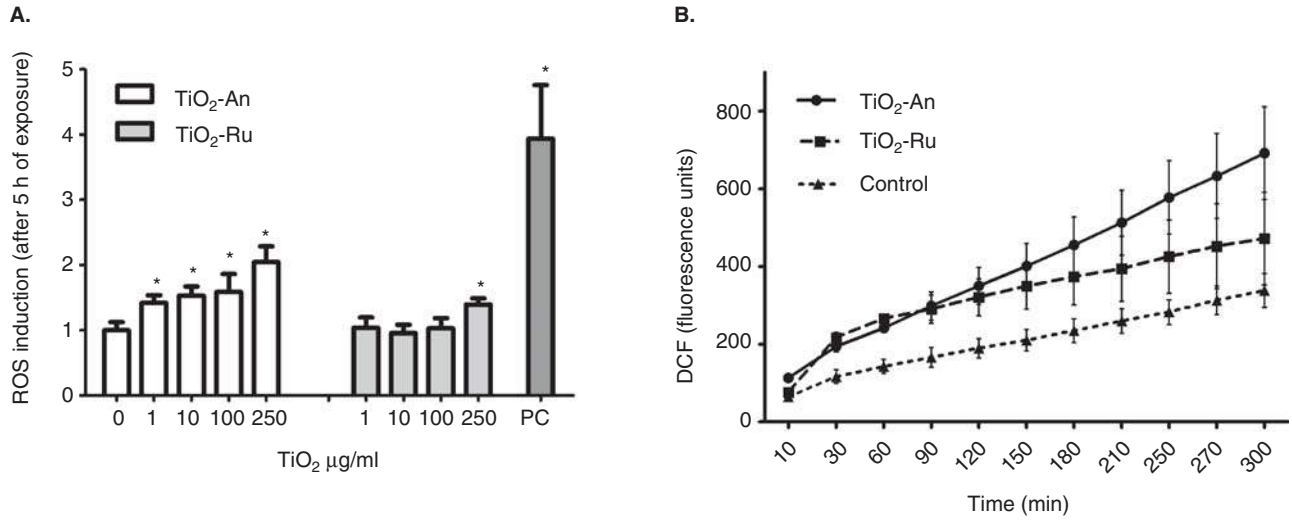

Figure 2. TiO_2-An and TiO_2-Ru NPs-induced intracellular ROS formation in HepG2 cells. (A) Induction of ROS formation presented as relative increase of DCF fluorescence after 5 h exposure to TiO_2 NPs, (B) kinetics of ROS formation during the 5 h exposure to 250 μg/ml TiO_2 NPs. The HepG2 cells loaded with DCFH-DA (20 μM/30 min) were exposed to graded doses of TiO_2-An and TiO_2-Ru NPs. DCF fluorescence intensity was measured at 30 min intervals during the 5 h incubation. (A) Each bar represent means (±SD) of three independent experiments, (B) each point represents the mean of five replicates (±SD) of representative experiment. (*) denotes a significant difference between TiO_2 NPs-treated groups and control (Student's *t*-test, $P < 0.05$).

gadd45α, whereas after 24 h exposure BaP induced 14-fold increase of the expression of *p21* and six-fold increase of the *gadd45α,* while the expression of *mdm2* and *p53* was not affected (data not shown). These data confirmed expected responsiveness of the system with HepG2 cells.

Discussion and conclusion

In this study, we have shown that in HepG2 cells genotoxic potential of TiO_2 NPs varies with particle size and crystalline structure. Neither TiO_2-An nor TiO_2-Ru affected the viability of HepG2 cells, which is in line with the recent report of Wagner et al. (2009). On the other hand, both types of TiO_2 NPs induced intracellular ROS formation, DNA strand breaks and oxidative DNA damage with TiO_2-An being significantly stronger inducer than TiO_2-Ru. For the first time we showed that exposure to TiO_2 NPs induced changes in the mRNA expression of DNA damage responsive genes, which is characteristic for genotoxic agents.

The TiO_2 powders used in this study differ in particles size as well as in crystalline structure, which could both contribute to the observed differences in their effects. As presented in Figures 1A–E, the particles are highly aggregated and agglomerated, which is in line with a number of previous studies (Limbach et al. 2005; Xia et al. 2006; Falck et al. 2009), and portion of submicron-sized agglomerates in TiO_2-An is much lower than in TiO_2-Ru. This implies that the observed more pronounced effects of the TiO_2-An could be partly ascribed to a higher concentration of the small particles. However, in our opinion supported by literature data, the role of crystalline structure can not be excluded.

For particles with low solubility, such as TiO_2, their capacity to produce ROS is generally proposed to account for their genotoxicity (Schins 2002; Schins and Knaapen 2007). In our experiments we confirmed that both types of TiO_2 NPs induced intracellular ROS formation, which is in agreement with other reports describing ROS induction in bronchial epithelial cells (Gurr et al. 2005; Hussain et al. 2009), lung epithelial cells (Limbach et al. 2005), and also brain microglia (Long et al. 2006). We also observed that the TiO_2-An was significantly stronger ROS inducer than TiO_2-Ru, which corroborates the results of Jiang et al. (2008). The difference in the intrinsic ability of anatase and rutile TiO_2 to induce ROS has been shown to be related to differences in their surface chemistry (Selloni et al. 1998; Vittadini et al. 1998).

TiO_2-An caused weak, however at all exposure times persistent increase in DNA strand breaks, and persistent dose-dependent increase in Fpg-sensitive sites, whereas TiO_2-Ru was practically ineffective (Figure 4). Similar observations have been reported in several previous studies (Gurr et al. 2005; Reeves et al. 2008; Zhu et al. 2009). The fact that TiO_2-An induced significant increase in the level of Fpg-sensitive sites, while Endo III-sensitive sites remained

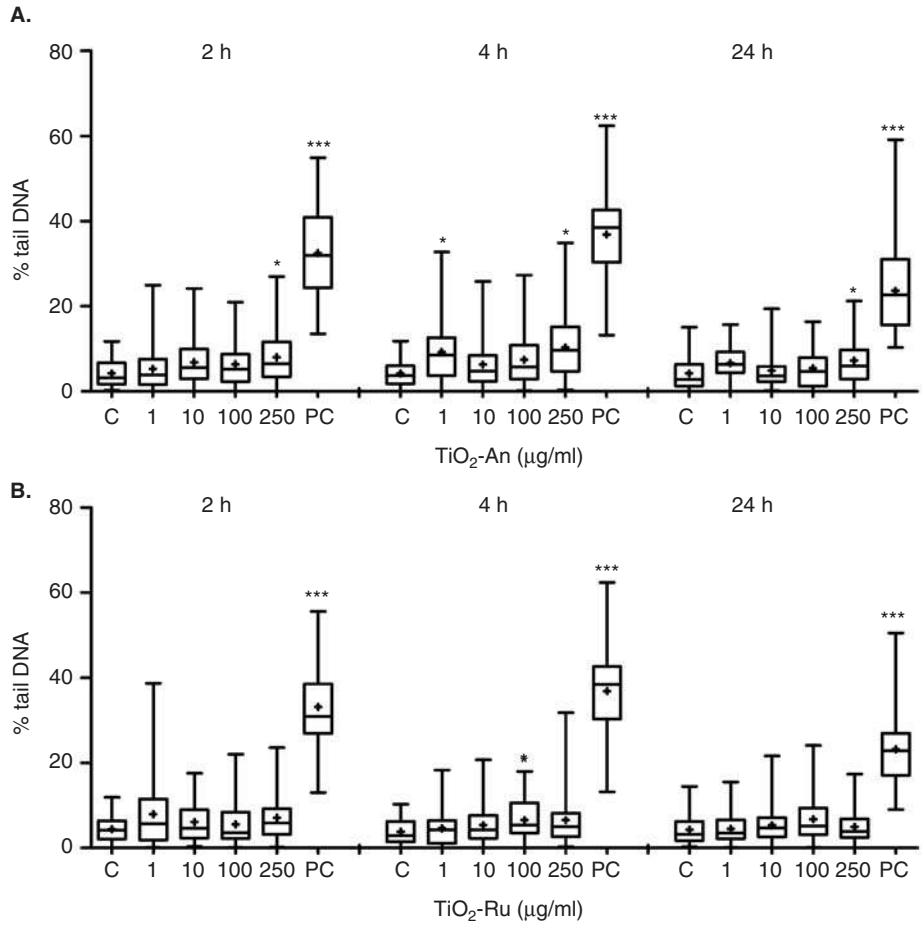

Figure 3. DNA strand break induction by TiO_2-An (A) and TiO_2-Ru (B) in HepG2 cells. The cells were treated for 2, 4 and 24 h with TiO_2 NPs (0, 1, 10, 100, 250 μg/ml). 0.5 mM *t*-BOOH was used as positive control for 2 and 4 h treatments and 50 μM BaP for 24 h treatments. The DNA damage was assessed using the comet assay as described in *Materials and methods,* and is expressed as % of DNA in the tail. Fifty cells were analyzed per experimental point in each of the three independent experiments. Data are presented as quantile box plots. The edges of the box represent the 25th and 75th percentiles, the median is a solid line through the box, mean values are represented as square (+), and the error bars represent the 95% confidence intervals. $^{*}P < 0.05$ and $^{***}P < 0.001$ denotes a significant difference between TiO_2 NPs-treated and control groups using ANOVA, Kruskal-Wallis with Dunnet's post test.

unchanged suggests that product of TiO_2-induced oxidative DNA damage is 8-hydroxyguanine (8-OH-Gua), although formamidopyrimidines (imidazole ring-opened purines) are also possible substrate for Fpg (Kielbassa et al. 1997). 8-OH-Gua adducts in DNA lead to GC → TA transversion mutations, unless repaired prior to DNA replication (Grollman and Moriya 1993; Olinski et al. 2002). Therefore, persistence of oxidized purines in cells may lead to mutations and cancer (Valko et al. 2006).

Toxicogenomics, the application of expression profiling in toxicological studies, has the potential to allow deeper understanding of the mechanisms of toxicity and can also provide an early and global answer to toxic events (Brown and Botstein 1999; Kolaja and Kramer 2002; Ulrich and Friend 2002; Ellinger-Ziegelbauer et al. 2005). In our study we have measured changes in the expression of four genes that are involved in response to DNA damage: *p53* and its downstream targets *p21, gadd45α,* and *mdm2.* p53 tumor suppressor is considered to be the major sensor of genotoxic stress and is the link between DNA damage, cell cycle arrest and apoptosis (Levine 1997). The up-regulation of *p53* gene after exposure to TiO_2-An and TiO_2-Ru was short-term. On the transcription level this is not unusual, as it is known that DNA damage activates the p53 protein, predominantly through its phosphorylation by DNA damage responsive kinases and, to a lesser extent, through up-regulation of gene expression (Zhou and Elledge 2000). Recently it has been reported that exposure of peripheral blood lymphocytes to TiO_2

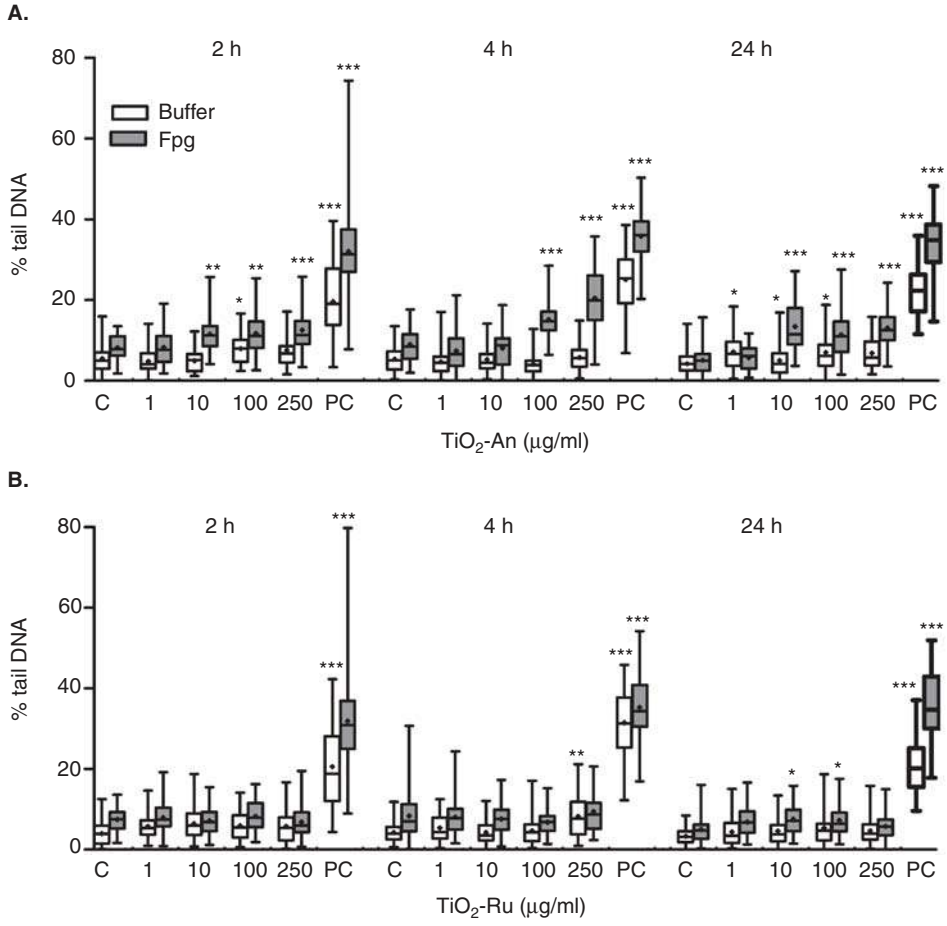

Figure 4. Induction of Fpg sensitive sites by TiO_2-An (A) and TiO_2-Ru (B) in HepG2 cells. The cells were exposed to TiO_2 NPs (0, 1, 10, 100 and 250 μg/ml) for 2, 4 and 24 h, then the modified comet assay was performed as described in *Materials and methods.* The levels of DNA strand breaks and oxidized purines are expressed as percent of tail DNA. Fifty cells were analyzed per experimental point in each of the two independent experiments. Data are presented as quantile box plots (for details see the caption of Figure 3). $*P < 0.05$, $**P < 0.01$ and $***P < 0.001$ denotes a significant difference between TiO_2 NPs-treated and control groups with and without Fpg, respectively, using ANOVA, Kruskal-Wallis with Dunnet's post test.

NPs (70–85% anatase/15–30% rutile) caused accumulation of p53 protein together with intracellular ROS generation, DNA damage and micronuclei formation (Kang et al. 2008). Under normal conditions the function of p53 is tightly regulated by its interaction with MDM2, an E3 ubiquitin ligase, which mediates ubiquitination of p53 and its proteosome-dependent degradation (Vogelstein et al. 2000). Expression of *mdm2* gene is itself regulated with an autoregulatory loop in which p53 positively regulates *mdm2* expression while MDM2 protein negatively regulates p53 levels and activity (Wu et al. 1993). Both types of TiO_2 NPs induced increased expression of *mdm2* gene, although TiO_2-Ru was the stronger. Ellinger-Ziegelbauer et al. (2005), who compared the profiles of gene expression induced by genotoxic and non-genotoxic carcinogens in rat liver, found that *mdm2* was specifically up-regulated by genotoxic carcinogens. Up-regulation of *mdm2* has been detected also after exposure of HepG2 cells to microcystine-LR, for which it has been shown to induce DNA damage via ROS formation (Zegura et al. 2008). Following DNA damage, the growth arrest and DNA damage gene *gadd45*α plays a role in controlling the cell cycle G2–M checkpoint, the DNA repair process and apoptosis (Zhan 2005). Induction of *gadd45*α is directly transcriptionally regulated by p53 and it has been reported to be associated with the oxidative stress-induced pathway (Wang et al. 1999). The *gadd45*α gene has been observed to be induced in response to a wide range of genotoxic agents, including BaP (Akerman et al. 2004), mitomycin C (Abbas et al. 2002), cisplatin (Smith et al. 1996), H_2O_2 (Fornace et al. 1988), microcystin-LR (Zegura et al. 2008), and organophosphorous pesticides (Hreljac et al. 2008). Significantly elevated

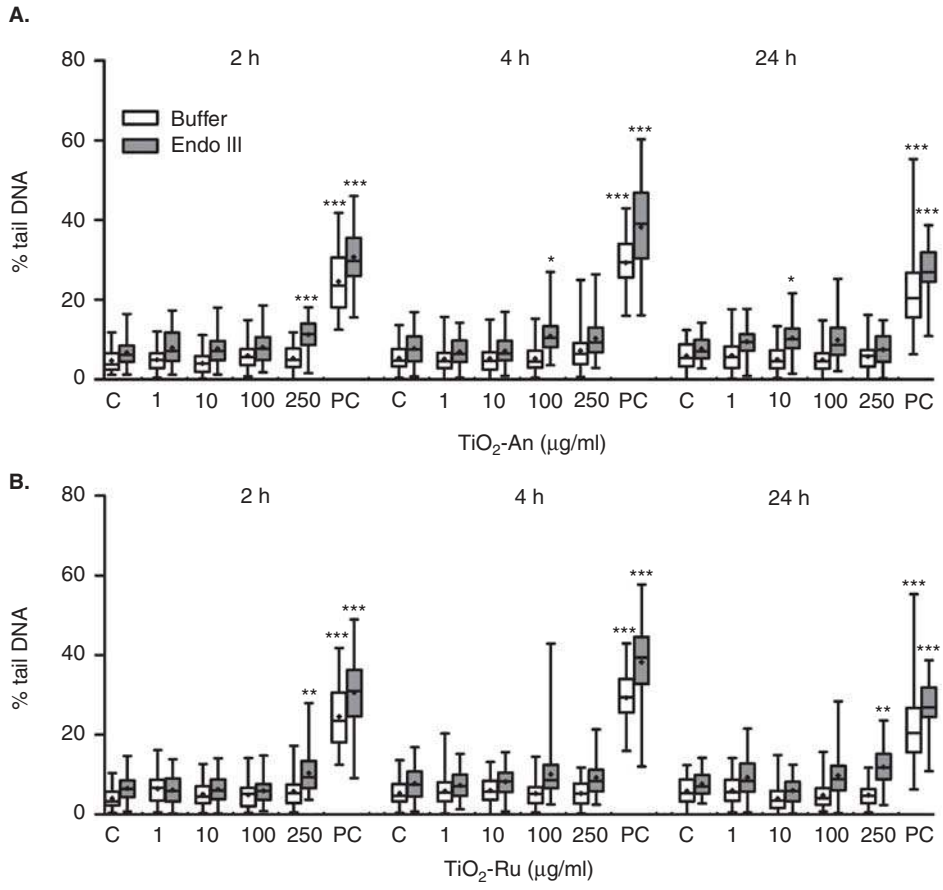

Figure 5. Induction of Endo III-sensitive sites by TiO_2-An (A) and TiO_2-Ru (B) in HepG2 cells. The cells were exposed to TiO_2 NPs (0, 1, 10, 100 and 250 μg/ml) for 2, 4 and 24 h, then the modified comet assay was performed as described in *Materials and methods.* The levels of DNA strand breaks and oxidized pyrimidines are expressed as percent of tail DNA. Fifty cells were analyzed per experimental point in each of the two independent experiments. Data are presented as quantile box plots (for details see the caption of Figure 3). $^{*}P < 0.05$, $^{**}P < 0.01$ and $^{***}P < 0.001$ denotes a significant difference between TiO_2 NPs-treated and control groups with and without Endo III, respectively, using ANOVA, Kruskal-Wallis with Dunnet's post test.

expression of *gadd45α* was induced by both types of TiO_2 NPs after 4 h and 24 h exposure, with TiO_2-Ru being the stronger inducer. Another p53 target is p21, a cyclin-dependent kinase inhibitor, which is responsible for cell cycle arrest following DNA damage (Waldman et al. 1995). TiO_2-Ru induced *p21* mRNA expression more strongly than TiO_2-An, as was observed also with *mdm2* and *gadd45α*. Ellinger-Ziegelbauer et al. (2005) found that, in rat liver, *p21* was exclusively up-regulated by genotoxic carcinogens.

Exposure of HepG2 cells to TiO_2-Ru NPs induced earlier and higher up-regulation of DNA damage responsive genes than exposure to TiO_2-An NPs. This appears to contradict the higher DNA damaging potential of TiO_2-An NPs observed with the comet assay. However, up-regulation of DNA damage responsive genes in fact reflects a cellular defense response against the consequences of DNA damage. Thus one possible explanation is that, in the cells exposed to TiO_2-Ru NPs, only marginal DNA damage was observed, because the early defense response triggered repair processes that eliminated the DNA damage before it could be detected with the comet assay.

In conclusion, exposure of HepG2 cells to TiO_2 NPs did not affect their viability, but induced increase in oxidative DNA damage, which was associated with intracellular ROS production. Exposure to TiO_2 NPs induced changes in the mRNA expression of *p53* and its downstream regulated DNA damage responsive genes *p21, gadd45α* and *mdm2,* providing additional evidence that TiO_2 NPs are genotoxic. The observed differences in the responses of HepG2 cells to exposure to TiO_2-An and TiO_2-Ru NPs supports evidence that the toxic potential of TiO_2 NPs depends not only on the size, but also on the crystalline structure.

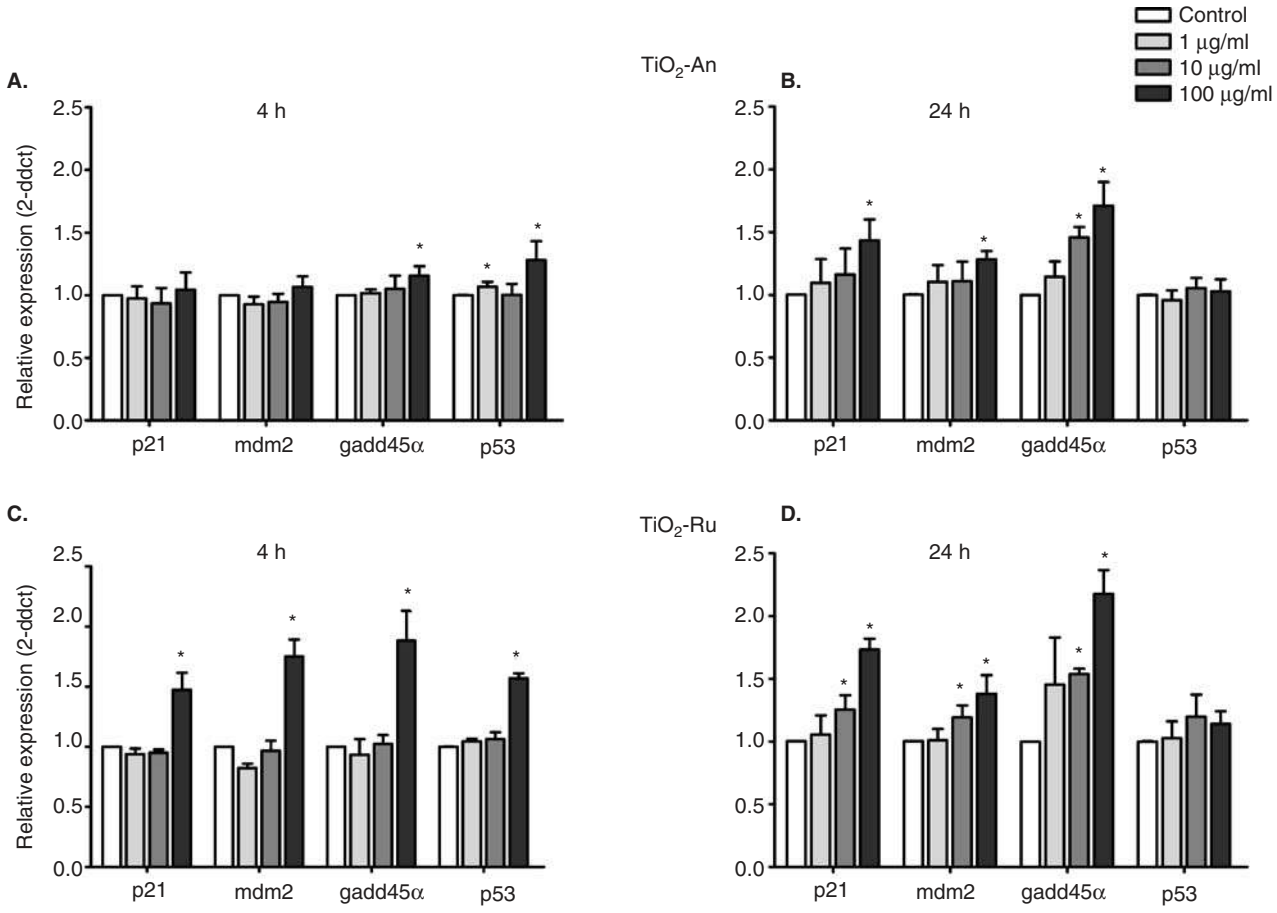

Figure 6. Real-time PCR analysis of the changes in *p53*, *mdm2*, *gadd45α* and *p21* gene expression after exposure of HepG2 cells to TiO_2-An for 4 h (A) and 24 h (B) and TiO_2-Ru after exposure for 4 h (C) and 24 h (D). The cells were exposed to TiO_2 NPs (0, 1, 10 and 100 μg/ml) for 4 and 24 h, then the RT-PCR was performed as described in *Materials and methods*. The results are expressed as relative mRNA expression normalized to untreated control. Duplicate experiments were repeated at least three times. (*) Denotes a significant difference between TiO_2 NPs-treated groups and control (Student's *t*-test; $P < 0.05$).

Acknowledgments

This study was supported by Slovenian Research Agency: Program P1-0245 and young researcher grant to JP. We also thank Dr Zoran Samardžija for FEG-SEM examination of the powders. We thank Anja Pucer for her valuable advice in technical support. We thank Professor Roger Pain for critical reading of the manuscript.

Declaration of interest: The authors report no conflict of interest. The authors alone are responsible for the content and writing of the paper.

References

Abbas T, Olivier M, Lopez J, Houser S, Xiao G, Kumar GS, Tomasz M, Bargonetti J. 2002. Differential activation of p53 by the various adducts of Mitomycin C. J Biol Chem 277:40513–40519.

Ackroyd R, Kelty C, Brown N, Reed M. 2001. The History of photodetection and photodynamic therapy. Photochem Photobiol 74:656–669.

Akerman GS, Rosenzweig BA, Domon OE, McGarrity LJ, Blankenship LR, Tsai CA, Culp SJ, MacGregor JT, Sistare FD, Chen JJ, et al. 2004. Gene expression profiles and genetic damage in benzo(a)pyrene diol epoxide-exposed TK6 cells. Mutat Res, Fundam Mol Mech Mutagen 549:43–64.

Baggs RB, Ferin J, Oberdörster G. 1997. Regression of pulmonary lesions produced by inhaled titanium dioxide in rats. Vet Pathol 34:592–597.

Bermudez E, Mangum JB, Asgharian B, Wong BA, Reverdy EE, Janszen DB, Hext PM, Warheit DB, Everitt JI. 2002. Long-term pulmonary responses of three laboratory rodent species to subchronic inhalation of pigmentary titanium dioxide particles. Toxicol Sci 70:86–97.

Bermudez E, Mangum JB, Wong BA, Asgharian B, Hext PM, Warheit DB, Everitt JI. 2004. Pulmonary responses of mice, rats, and hamsters to subchronic inhalation of ultrafine titanium dioxide particles. Toxicol Sci 77:347–357.

Bernard BK, Osheroff MR, Hofmann A, Mennear JH. 1990. Toxicology and carcinogenesis studies of dietary titanium dioxide-coated mica in male and female Fischer 344 rats. J Toxicol Environ Health 29:417–429.

Borm PJA, Hohr D, Steinfartz Y, Zeittrager I, Albrecht C. 2000. Chronic inflammation and tumor formation in rats after intratracheal instillation of high doses of coal dusts, titanium dioxides, and quartz. Inhalation Toxicol 12:225–231.

Brown PO, Botstein D. 1999. Exploring the new world of the genome with DNA microarrays. Nat Genet 21:33–37.

Chen JL, Fayerweather WE. 1988. Epidemiologic study of workers exposed to titanium dioxide. J Occup Med 30:937–942.

Cho M, Chung H, Choi W, Yoon J. 2004. Linear correlation between inactivation of E. coli and OH radical concentration in TiO2 photocatalytic disinfection. Water Res 38:1069–1077.

Collins AR, Dusinska M, Gedik CM, Stetina R. 1996. Oxidative damage to DNA: Do we have a reliable biomarker? Environ Health Perspect 104(3):465–469.

Dunford R, Salinaro A, Cai L, Serpone N, Horikoshi S, Hidaka H, Knowland J. 1997. Chemical oxidation and DNA damage catalysed by inorganic sunscreen ingredients. FEBS Lett 418:87–90.

Ellinger-Ziegelbauer H, Stuart B, Wahle B, Bomann W, Ahr HJ. 2005. Comparison of the expression profiles induced by genotoxic and nongenotoxic carcinogens in rat liver. Mutat Res 575:61–84.

Fabian E, Landsiedel R, Ma-Hock L, Wiench K, Wohlleben W, van Ravenzwaay B. 2008. Tissue distribution and toxicity of intravenously administered titanium dioxide nanoparticles in rats. Arch Toxicol 82:151–157.

Falck GC, Lindberg HK, Suhonen S, Vippola M, Vanhala E, Catalan J, Savolainen K, Norppa H. 2009. Genotoxic effects of nanosized and fine TiO2. Hum Exp Toxicol 28:339–352.

Fornace AJ, Alamo I, Hollander MC. 1988. DNA damage-inducible transcripts in mammalian cells. Proc Natl Acad Sci USA 85:8800–8804.

Gelis C, Girard S, Mavon A, Delverdier M, Paillous N, Vicendo P. 2003. Assessment of the skin photoprotective capacities of an organo-mineral broad-spectrum sunblock on two ex vivo skin models. Photodermatol Photoimmunol Photomed 19:242–253.

Grassian VH, O'shaughnessy PT, Adamcakova-Dodd A, Pettibone JM, Thorne PS. 2007. Inhalation exposure study of titanium dioxide nanoparticles with a primary particle size of 2 to 5 nm. Environ Health Perspect 115:397–402.

Greenwood NN, Earnshaw A. 1997. Chemistry of the elements. 2nd ed. Oxford: Butterworth-Heinemann.

Grollman AP, Moriya M. 1993. Mutagenesis by 8-oxoguanine: An enemy within. Trends Genet 9:246–249.

Gurr JR, Wang AS, Chen CH, Jan KY. 2005. Ultrafine titanium dioxide particles in the absence of photoactivation can induce oxidative damage to human bronchial epithelial cells. Toxicology 213:66–73.

Hart GA, Hesterberg TW. 1998. In vitro toxicity of respirable-size particles of diatomaceous earth and crystalline silica compared with asbestos and titanium dioxide. J Occup Environ Med 40:29–42.

Hohr D, Steinfartz Y, Schins RPF, Knaapen AM, Martra G, Fubini B, Borm PJA. 2002. The surface area rather than the surface coating determines the acute inflammatory response after instillation of fine and ultrafine TiO2 in the rat. Int J Hyg Environ Health 205:239–244.

Hreljac I, Zajc I, Lah T, Filipic M. 2008. Effects of model organophosphorous pesticides on DNA damage and proliferation of HepG2 cells. Environ Mol Mutagen 49:360–367.

Hussain S, Boland S, Baeza-Squiban A, Hamel R, Thomassen LCJ, Martens JA, Billon-Galland MA, Fleury-Feith J, Moisan F, Pairon J-C, et al. 2009. Oxidative stress and proinflammatory effects of carbon black and titanium dioxide nanoparticles: Role of particle surface area and internalized amount. Toxicology 260:142–149.

Hussain SM, Hess KL, Gearhart JM, Geiss KT, Schlager JJ. 2005. In vitro toxicity of nanoparticles in BRL 3A rat liver cells. Toxicol In Vitro 19:975–983.

International Agency for Research on Cancer (IARC). 2006. Monographs on the evaluation of carcinogenic risks to humans. Vol. 93. Lyon, France: IARC. Accessed 6 February 2009 from the website: http://monographs.iarc.fr/ENG/Meetings/93-titaniumdioxide.pdf.

Jiang J, Oberdörster G, Elder A, Gelein R, Mercer P, Biswas P. 2008. Does nanoparticle activity depend upon size and crystal phase? Nanotoxicology 2:33–42.

Kang SJ, Kim BM, Lee YJ, Chung HW. 2008. Titanium dioxide nanoparticles trigger p53-mediated damage response in peripheral blood lymphocytes. Environ Mol Mutagen 49:399–405.

Kielbassa C, Roza L, Epe B. 1997. Wavelength dependence of oxidative DNA damage induced by UV and visible light. Carcinogenesis 18:811–816.

Kolaja KL, Kramer JA. 2002. Toxicogenomics: An opportunity to optimise drug development and safety evaluation. Expert Opin Drug Saf 1:275–286.

LeBel CP, Ischiropoulos H, Bondy SC. 1992. Evaluation of the probe 2′,7′-dichlorofluorescin as an indicator of reactive oxygen species formation and oxidative stress. Chem Res Toxicol 5:227–231.

Levine AJ. 1997. p53, the cellular gatekeeper for growth and division. Cell 88:323–331.

Limbach LK, Li Y, Grass RN, Brunner TJ, Hintermann MA, Muller M, Gunther D, Stark WJ. 2005. Oxide nanoparticle uptake in human lung fibroblasts: Effects of particle size, agglomeration, and diffusion at low concentrations. Environ Sci Technol 39:9370–9376.

Lomer MC, Thompson RP, Powell JJ. 2002. Fine and ultrafine particles of the diet: Influence on the mucosal immune response and association with Crohn's disease. Proc Nutr Soc 61:123–130.

Long TC, Saleh N, Tilton RD, Lowry GV, Veronesi B. 2006. Titanium dioxide (P25) produces reactive oxygen species in immortalized brain microglia (BV2): Implications for nanoparticle neurotoxicity. Environ Sci Technol 40:4346–4352.

Mossman T. 1983. Rapid colorimetric assay for cellular growth and survival: Application to proliferation and cytotoxicity assays. J Immunol Methods 65:55–63.

Nordman H, Berlin M. 1986. Titanium. In: Friberg L, Nordberg GF, Vouk VB, editors. Handbook on the toxicology of metals. Vol. II. Amsterdam: Elsevier. pp 595–609.

Olinski R, Gackowski D, Foksinski M, Rozalski R, Roszkowski K, Jaruga P. 2002. Oxidative DNA damage: Assessment of the role in carcinogenesis, atherosclerosis, and acquired immunodeficiency syndrome. Free Radic Biol Med 33:192–200.

Osseni RA, Debbasch C, Christen MO, Rat P, Warnet JM. 1999. Tacrine-induced reactive oxygen species in a human liver cell line: The role of anethole dithiolethione as a scavenger. Toxicol in Vitro 13:683–688.

Park E-J, Yoon J, Choi K, Yi J, Park K. 2009. Induction of chronic inflammation in mice treated with titanium dioxide nanoparticles by intratracheal instillation. Toxicology 260:37–46.

Rahman Q, Lohani M, Dopp E, Pemsel H, Jonas L, Weiss DG, Schiffmann D. 2002. Evidence that ultrafine titanium dioxide induces micronuclei and apoptosis in Syrian hamster embryo fibroblasts. Environ Health Perspect 110:797–800.

Powder diffraction files (International Centre for Diffraction Data): JCPDS card numbers 34–0180 and 21-1272.

Reeves JF, Davies SJ, Dodd NJF, Jha AN. 2008. Hydroxyl radicals (OH) are associated with titanium dio.

xide (TiO2) nanoparticle-induced cytotoxicity and oxidative DNA damage in fish cells. Mutat Res, Fundam Mol Mech Mutagen 640:113–122.

Schins RP. 2002. Mechanisms of genotoxicity of particles and fibers. Inhal Toxicol 14:57–78.

Schins RP, Knaapen AM. 2007. Genotoxicity of poorly soluble particles. Inhal Toxicol 19 (1):189–198.

Selloni A, Vittadini A, Grätzel M. 1998. The adsorption of small molecules on the TiO2 anatase (101) surface by first-principles molecular dynamics. Surf Sci 402(404):219–222.

Singh NP, McCoy MT, Tice RR, Schneider EL. 1988. A simple technique for quantitation of low levels of DNA damage in individual cells. Exp Cell Res 175:184–191.

Smith ML, Kontny HU, Zhan Q, Sreenath A, O'Connor PM, Fornace AJ Jr. 1996. Antisense GADD45 expression results in decreased DNA repair and sensitizes cells to U.V.-irradiation or cisplatin. Oncogene 13:2255–2263.

Tryba B. 2008. Increase of the photocatalytic activity of TiO2 by carbon and iron modifications. Int J Photoenergy 8:1–15.

Ulrich R, Friend SH. 2002. Toxicogenomics and drug discovery: Will new technologies help us produce better drugs? Nat Rev Drug Discov 1:84–88.

Valko M, Rhodes CJ, Moncol J, Izakovic M, Mazur M. 2006. Free radicals, metals and antioxidants in oxidative stress-induced cancer. Chem-Biol Interact 160:1–40.

Vittadini A, Selloni A, Rotzinger FP, Grätzel M. 1998. Structure and energetics of water adsorbed at TiO2 anatase\(101\) and \(001\) surfaces. Phys Rev Lett 81(14):2954–2957.

Vogelstein B, Lane D, Levine AJ, 2000. Surfing the p53 network. Nature 408:307–310.

Wagner S, Münzer S, Behrens P, Scheper T, Bahnemann D, Kasper C. 2009. Cytotoxicity of titanium and silicon dioxide nanoparticles. J Phys Conf Ser 170(1):012022.

Waldman T, Kinzler KW, Vogelstein B. 1995. p21 is necessary for the p53-mediated G1 arrest in human cancer cells. Cancer Res 55:5187–5190.

Wang J, Zhou G, Chen C, Yu H, Wang T, Ma Y, Jia G, Gao Y, Li B, Sun J, et al. 2007a. Acute toxicity and biodistribution of different sized titanium dioxide particles in mice after oral administration. Toxicol Lett 168:176–185.

Wang JJ, Sanderson BJ, Wang H. 2007b. Cyto- and genotoxicity of ultrafine TiO2 particles in cultured human lymphoblastoid cells. Mutat Res 628:99–106.

Wang XW, Zhan Q, Coursen JD, Khan MA, Kontny HU, Yu L, Hollander MC, Connor PM, Fornace AJ, Harris CC. 1999. GADD45 induction of a G2/M cell cycle checkpoint. Proc Natl Acad Sci USA 96:3706–3711.

Warheit DB, Webb TR, Sayes CM, Colvin VL, Reed KL. 2006. Pulmonary instillation studies with nanoscale TiO2 rods and dots in rats: Toxicity is not dependent upon particle size and surface area. Toxicol Sci 91:227–236.

Wu X, Bayle JH, Olson D, Levine AJ. 1993. The p53-mdm-2 autoregulatory feedback loop. Genes Dev 7:1126–1132.

Xia T, Kovochich M, Brant J, Hotze M, Sempf J, Oberley T, Sioutas C, Yeh JI, Wiesner MR, Nel AE. 2006. Comparison of the abilities of ambient and manufactured nanoparticles to induce cellular toxicity according to an oxidative stress paradigm. Nano Lett 6:1794–1807.

Zegura B, Lah TT, Filipic M. 2004. The role of reactive oxygen species in microcystin-LR-induced DNA damage. Toxicology 200:59–68.

Zegura B, Sedmak B, Filipic M. 2003. Microcystin-LR induces oxidative DNA damage in human hepatoma cell line HepG2. Toxicon 41:41–48.

Zegura B, Zajc I, Lah TT, Filipic M, 2008. Patterns of microcystin-LR induced alteration of the expression of genes involved in response to DNA damage and apoptosis. Toxicon 51: 615–623.

Zhan Q. 2005. Gadd45a, a p53- and BRCA1-regulated stress protein, in cellular response to DNA damage. Mutat Res, Fundam Mol Mech Mutagen 569:133–143.

Zhang AP, Sun YP. 2004. Photocatalytic killing effect of TiO2 nanoparticles on Ls-174-t human colon carcinoma cells. World J Gastroenterol 10:3191–3193.

Zhou BB, Elledge SJ. 2000. The DNA damage response: Putting checkpoints in perspective. Nature 408:433–439.

Zhu RR, Wang SL, Chao J, Shi DL, Zhang R, Sun XY, Yao SD. 2009. Bio-effects of Nano-TiO2 on DNA and cellular ultrastructure with different polymorph and size. Mater Sci Eng C 29:691–696.

Žegura B, Filipič M. 2004. Application of in vitro comet assay for genotoxicity testing. In: Zhengyin Y, Caldwell GW, editors. Methods in pharmacology and toxicology, optimization in drug discovery: In vitro methods. Totowa: Humana Press. pp 301–313.